Planetary and Gravity Waves in a Polar Basin

ANDREW J. WILLMOTT AND ESTANISLAO GAVILAN PASCUAL-AHUIR

Newcastle University, Newcastle upon Tyne, United Kingdom

(Manuscript received 11 November 2016, in final form 7 March 2017)

ABSTRACT

The eigenfrequencies of freely propagating barotropic, divergent, planetary waves and gravity waves in a spherical polar cap are presented using an approximation in which full spherical geometry is retained in the derivation of the wave amplitude equation. Subsequently, the colatitude angle in the coefficients of the wave amplitude equation is fixed, thereby allowing the eigenvalue problem to be solved using analytical methods. The planetary wave frequencies are compared with published results that adopt the polar-plane approximation to solve the equivalent free-wave problem. Low-order planetary wave frequencies calculated in this study agree well with the polar-plane approximation results. The sensitivity of the wave frequencies to the choice of the fixed colatitude in the coefficients of the wave amplitude equation is discussed.

1. Introduction

The analytical treatment of atmospheric or oceanic dynamics in a polar basin centered at the pole is hindered by the nonuniform meridional gradient of the Coriolis parameter. LeBlond (1964) illustrates this point in developing the polar-plane approximation. The Coriolis parameter $f = 2\Omega\cos\theta$, where Ω is the angular velocity of the rotation of Earth and θ is the colatitude. In terms of plane polar coordinates r, φ in the plane of projection, tangent to Earth at the pole, we observe that

$$\begin{aligned} f &= 2\Omega\left(1-\frac{\theta^2}{2}+\ldots\right), \\ &= 2\Omega\left[1-\frac{1}{2}\left(\frac{r}{R}\right)^2+\ldots\right], \end{aligned} \tag{1.1}$$

where R is the radius of Earth. For dynamics on the polar plane with horizontal length scales satisfying the constraint

$$\left(\frac{r}{R}\right)^2 \ll 1,$$

LeBlond (1964) introduces the approximation

$$\begin{aligned} f &\approx 2\Omega, \\ \frac{df}{dr} &\approx -\frac{2\Omega r}{R^2}, \end{aligned}$$

which follows immediately from (1.1). Therefore, starting with one of the simplest analogs for a polar ocean on a polar plane, namely, a homogeneous fluid, we predict that the barotropic potential vorticity equation will have nonconstant coefficients. Nevertheless, LeBlond (1964) obtains the dispersion relation for divergent barotropic planetary waves in a flat bottom polar basin. In related meteorological studies, Haurwitz (1975) and Bridger and Stevens (1980) use cylindrical polar coordinates to study freely propagating waves in a high-latitude atmosphere. The concept of the delta (δ)-plane approximation for quasigeostrophic dynamics at high latitudes was developed by Harlander (2005). Harlander (2005) demonstrates that the high-latitude δ-plane model can be consistently derived from spherical geometry. On the δ plane, Harlander (2005) demonstrates that high-latitude Rossby waves' energy rays are curved, which is not the case on the β plane.

In contrast with studies of free waves in a polar basin, there is a considerable body of literature on free waves in a thin layer of fluid on the entire rotating Earth. For example, Paldor et al. (2013) and Paldor (2015) obtain solutions for zonally propagating planetary and inertial-gravity (i.e., Poincaré) waves on the entire rotating Earth, extending the solutions in the seminal work of Longuet-Higgins (1968).

In this paper, we present a new method for obtaining the dispersion relation for freely propagating barotropic gravity and planetary waves in a polar basin. The

Corresponding author: Andrew J. Willmott, andrew.willmott@newcastle.ac.uk

DOI: 10.1175/JPO-D-16-0253.1

computationally efficient dispersion relation is derived using a somewhat overlooked approximation first proposed by Imawaki and Takano (1974) in their analysis of source–sink-driven planetary geostrophic dynamics in a polar basin. E. Gavilan Pascual-Ahuir (2017, unpublished manuscript) uses the Imawaki and Takano (1974) (IT) approximation to analytically derive solutions for planetary geostrophic steady circulation driven by prescribed inflow/outflow at the boundary of a circular basin with simple shelf topography. We will hereinafter adopt the phrase "IT approximation," in which the linearized spherical shallow-water equations are used to derive the barotropic vorticity equation, and thereafter the colatitude is fixed in the coefficients of this partial differential equation, an approach first discussed by Imawaki and Takano (1974) as far as the authors are aware. How well does the IT approximation capture the dynamics of freely propagating gravity and divergent planetary waves in a polar basin? This question is addressed in this paper, which is structured as follows: Section 2 derives the eigenvalue problem for gravity and planetary waves using the IT approximation. Subsequently, planetary waves are discussed in section 3, and gravity waves are discussed in section 4, followed by conclusions in section 5.

2. Formulation of the eigenvalue problem

We consider an ocean of uniform density on a polar cap with a center located at the pole. A spherical polar coordinates system is adopted where θ and φ denote the colatitude and longitude angles, respectively. Let θ_B denote the colatitude of the boundary of the polar basin. Then, $\theta \in [0, \theta_B)$ and $\varphi \in [0, 2\pi)$. The unit vectors $(\mathbf{k}, \hat{\boldsymbol{\theta}}, \hat{\boldsymbol{\varphi}})$ form a right-handed triad, where

$$\mathbf{k} \wedge \hat{\boldsymbol{\theta}} = \hat{\boldsymbol{\varphi}},$$

and $\mathbf{k}$ is a unit vector in the (outward) radial direction (see Fig. 1). With respect to this coordinates system, the linearized shallow-water equations for inviscid homogeneous dynamics in the polar cap take the form

$$u_t + fv = -\frac{g}{R\sin\theta}\eta_\varphi, \tag{2.1a}$$

$$v_t - fu = -\frac{g}{R}\eta_\theta, \quad \text{and} \tag{2.1b}$$

$$\eta_t + \frac{1}{R\sin\theta}[(Hu)_\varphi + (Hv\sin\theta)_\theta] = 0, \tag{2.1c}$$

where the velocity $\mathbf{u} = u\hat{\varphi} + v\hat{\boldsymbol{\theta}}$; η is the free-surface elevation; H is the undisturbed depth of the ocean; and g is

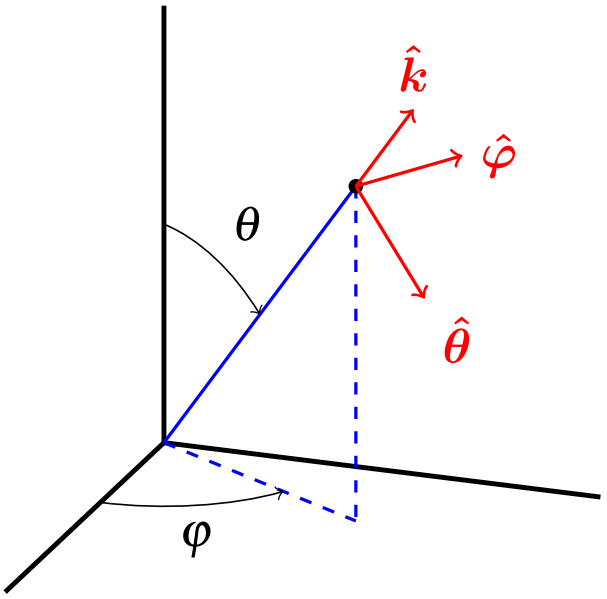

FIG. 1. Schematic of the spherical polar coordinate system showing the unit vectors $\hat{\mathbf{k}}$, $\hat{\boldsymbol{\theta}}$, and $\hat{\boldsymbol{\varphi}}$ that form a right-handed triad.

the gravitational acceleration. We seek azimuthally propagating wave solutions of (2.1) of the form

$$\left.\begin{aligned} u &= U(\theta)\exp[i(m\varphi - \omega t)] \\ v &= V(\theta)\exp[i(m\varphi - \omega t)] \\ \eta &= F(\theta)\exp[i(m\varphi - \omega t)] \end{aligned}\right\}, \tag{2.2}$$

where $\omega > 0$ is the angular wave frequency, m is the azimuthal integer wavenumber (i.e., $m = \pm 1, \pm 2, \pm 3, \ldots$), and U, V, and F are amplitude functions. Substituting (2.2) into (2.1), we obtain

$$-i\omega U + fV = -\frac{img}{R\sin\theta}F, \tag{2.3a}$$

$$-i\omega V - fU = -\frac{g}{R}F', \quad \text{and} \tag{2.3b}$$

$$-i\omega F + \frac{1}{R\sin\theta}[imHU + (HV\sin\theta)_\theta] = 0, \tag{2.3c}$$

where $F' \equiv dF/d\theta$. From (2.3a) and (2.3b), we find that

$$U = \frac{g\left(fF' - \dfrac{m\omega}{\sin\theta}F\right)}{R\mathcal{D}}, \quad \text{and} \tag{2.4a}$$

$$V = \frac{ig\left(\omega F' - \dfrac{mf}{\sin\theta}F\right)}{R\mathcal{D}}, \tag{2.4b}$$

where $\mathcal{D} \equiv f^2 - \omega^2$. Upon substituting (2.4) into (2.3c), and after some lengthy algebra, we obtain the wave amplitude equation for freely propagating waves in the polar cap:

$$F'' + \left(\frac{\sin 2\theta}{\cos^2\theta - \sigma^2} + \cot\theta\right)F' - \left[\frac{m}{\sigma}\left(\frac{\cos^2\theta + \sigma^2}{\cos^2\theta - \sigma^2}\right) + \frac{m^2}{\sin^2\theta} + \left(\frac{R}{r_e}\right)^2(\cos^2\theta - \sigma^2)\right]F = 0, \tag{2.5a}$$

where

$$\sigma = \frac{\omega}{2\Omega}, \quad r_e^2 = \frac{gH}{4\Omega^2}. \tag{2.5b}$$

We note that σ is the dimensionless wave frequency and that r_e is the external Rossby radius of deformation. On the basin wall we demand that there is no normal flow:

$$V = 0 \quad \text{on} \quad \theta = \theta_B,$$

which can be expressed as

$$F' - \frac{m}{\sigma}\cot\theta F = 0, \quad \text{on} \quad \theta = \theta_B, \tag{2.6}$$

upon using (2.4b). At the pole (2.5a) reduces to

$$F(0) = 0. \tag{2.7}$$

We now invoke the IT approximation and let $\theta = \theta_0$, where $0 < \theta_0 < \theta_B$ in the coefficients of (2.5a), thereby obtaining a constant coefficient, second-order, ordinary differential equation. Typically, we let $\theta_0 = 0.5\theta_B$, but the sensitivity of the free-wave dispersion relations to this angle will be discussed later. Equation (2.5a), together with boundary conditions (2.6) and (2.7), form a Sturm–Liouville eigenvalue problem for σ.

Before analyzing this eigenvalue problem in the subsequent sections, it is instructive to consider how the amplitude equation (2.5a) is modified when variations of f with colatitude are suppressed. An approximation of this type in a spherical polar basin would be valid for small wavelength waves in the meridional directions. When $f = 2\Omega$, the amplitude equation simplifies to

$$F'' + \cot\theta F' - \left[\frac{m^2}{\sin^2\theta} + \left(\frac{R}{r_e}\right)^2(1 - \sigma^2)\right]F = 0. \tag{2.8}$$

Comparing (2.8) with (2.5a), we observe that

$$\frac{\sin 2\theta}{\cos^2\theta - \sigma^2}; \quad \frac{m}{\sigma}\left(\frac{\cos^2\theta + \sigma^2}{\cos^2\theta - \sigma^2}\right)$$

arise from the variation of the Coriolis parameter with colatitude. On the f sphere, we noted that $f = 2\Omega$ (retaining the first term in the Maclaurin expansion in powers of θ), which leads to the modification of the term involving r_e in (2.5a).

3. Planetary waves ($\sigma^2 \ll 1$)

For these low-frequency waves, (2.5a) can be approximated as

$$F'' + AF' - BF = 0, \tag{3.1}$$

where

$$A \equiv 2\tan\theta_0 + \cot\theta_0 > 0$$

and

$$B \equiv \frac{m}{\sigma} + \frac{m^2}{\sin\theta_0} + \left(\frac{R}{r_e}\right)^2\cos^2\theta_0.$$

We observe that if the meridional structure of these wave modes is to be oscillatory then we require $m < 0$. The general solution of (3.1) will then take the form

$$F = \exp\left(-\frac{1}{2}A\theta\right)[c_1\cos(\kappa\theta) + c_2\sin(\kappa\theta)], \tag{3.2}$$

where

$$\kappa^2 = -B - (1/4)A^2,$$

and c_1 and c_2 are arbitrary constants. Notice that since $m < 0$, (2.2) reveals that the phase velocity of the waves is westward (i.e., in the negative φ sense), as expected for planetary waves. Application of (2.6) and (2.7) to (3.2) yields the dispersion relation for divergent barotropic planetary waves in spherical cap using the IT approximation:

$$\kappa = \left[\frac{m}{\sigma}\cot\theta_B + \frac{1}{2}A\right]\tan(\kappa\theta_B). \tag{3.3}$$

For a given value of m (<0), the discrete set of roots $\sigma_{m,n}(n = 1, 2, 3, \ldots)$ can be determined numerically from (3.3). However, approximate values of the roots are readily obtained from (3.3) upon noting that when $\sigma \ll 1$, the dispersion relation can be approximated by

$$m\cot\theta_B\tan(\kappa\theta_B) = 0,$$

from which

$$\kappa_n \approx \frac{n\pi}{\theta_B}, \quad n = 1, 2, \ldots. \tag{3.4}$$

TABLE 1. Parameter values used by LeBlond (1964) and also employed in this study.

Symbol	Variable (unit)	Value
Ω	Angular velocity of Earth (s^{-1})	7.292×10^{-5}
R	Radius of Earth (m)	6.370×10^{-6}
g	Gravitational acceleration ($m\,s^{-2}$)	9.8
H	Depth of the basin (m)	5753
θ_B	Colatitude at the boundary (°)	12.92

TABLE 2. Eigenfrequencies $\sigma_{m,n}$ determined from the full dispersion relation [(3.3)].

	$m = -1$	-2	-3	-4
$n = 1$	0.003 25	0.003 67	0.003 19	0.002 68
2	0.001 12	0.001 78	0.001 97	0.001 93
3	0.000 54	0.000 95	0.001 20	0.001 31
4	0.000 31	0.000 58	0.000 78	0.000 91
5	0.000 20	0.000 38	0.000 54	0.000 65

Using the expression for κ, (3.4) yields the approximate values for $\sigma_{m,n}$:

$$\frac{|m|}{\sigma_{m,n}} = \left(\frac{n\pi}{\theta_B}\right)^2 + \frac{m^2}{\sin^2\theta_0} + \left(\frac{R}{r_e}\right)^2 \cos^2\theta_0 + \sec^2\theta_0 + (1/4)\cot^2\theta_0. \tag{3.5}$$

Table 2 (below) presents the wave frequencies calculated from (3.3) using the ocean basin parameters in LeBlond (1964), which are listed in Table 1. In this study we do not explicitly use the radius r_B of the basin as a parameter in contrast with the polar-plane analysis of LeBlond (1964). However, $r_B = R\sin\theta_B$, and using the parameters in Table 1 we find that $r_B = 1424$ km. We find that the eigenfrequencies [(3.5)] are identical to those in Table 2 with the exception of $\sigma_{-1,1}$, which differs in the last decimal place. We observe from Table 3 that the low-order planetary wave modes are accurately represented using the IT approximation. More specially, $\sigma_{-1,n}$ ($n = 1, \ldots, 5$) and $\sigma_{-2,1}$ satisfying (3.3) are within 11% of the equivalent frequencies calculated by LeBlond (1964). We also observe increasing discrepancies between the eigenfrequencies determined by LeBlond (1964) and the IT approximation as the azimuthal and meridional wavelengths decrease, corresponding to increasing $|m|$ and n. This discrepancy reflects the fact that as the wavelengths of the modes decrease, their structure becomes more sensitive to the choice of the colatitude θ_0 in the dispersion relation. In practice, forced planetary waves generally have most of their energy in the lowest modes for which (3.5) gives accurate predictions for the wave periods. The planetary wave periods $T_{m,n} = \pi(\Omega\sigma_{m,n})^{-1}$ and for the gravest mode $\sigma_{-1,1} = 153$ days using $\sigma_{-1,1}$ in Table 2. The structure of the eigenfunctions is qualitatively identical to those in LeBlond (1964) and is therefore not reproduced here.

Figure 2 shows a plot of $\sigma_{-1,n}$ ($n = 1, \ldots, 5$) as a function of $\varepsilon^2 = (r_e/R)^2$, when $\theta_0 = 0.5\theta_B$. Varying ε is equivalent to varying the depth H of the ocean. The planetary wave frequencies in a polar basin are monotonic functions of ε. Similar qualitative behavior for the planetary wave eigenfrequencies on a sphere was noted by Longuet-Higgins (1968). Note that the asymptotic values of the eigenfrequencies $\sigma_{-1,n}$, in the limit of large H, are given by

$$\sigma_{-1,n} \to \left[\left(\frac{n\pi}{\theta_B}\right)^2 + \frac{1}{\sin^2\theta_0} + \sec^2\theta_0 + (1/4)\cot^2\theta_0\right]^{-1}.$$

How sensitive are the eigenfrequencies that are accurately approximated by the dispersion relation [(3.3)] to the value of θ_0? It is clear from (3.5) that for large $|m|$ and n the sensitivity of the eigenfrequencies to the values of these modal numbers will be small. To quantify this assertion, Table 4 shows $|\sigma_{m,n}(0.75\theta_B) - \sigma_{m,n}(0.5\theta_B)|/\sigma_{m,n}(0.5\theta_B)$, expressed as a percentage. Entries below the principal diagonal in Table 4 show decreasing sensitivity of the eigenvalues to the value of θ_0. In practice, we are interested in the sensitivity of $\sigma_{-1,n}$ ($n = 1, \ldots, 5$) and $\sigma_{-2,1}$ to θ_0 because they are a good approximation to the exact values. Clearly, the gravest mode eigenfrequency given by (3.5) provides an accurate approximation to the exact value when $\theta_0 = 0.5\theta_B$. Other values of $\theta_0 \in (0, \theta_B]$ reduce the accuracy of this frequency. On the other hand, $\sigma_{-1,4}$ and $\sigma_{-1,5}$ are relatively insensitive to θ_0 and provide acceptable approximations to their exact values. A final remark about the choice of θ_0 is that an alternative measure of frequency sensitivity to this angle is $|\sigma_{m,n}(0.25\theta_B) - \sigma_{m,n}(0.5\theta_B)|/\sigma_{m,n}(0.5\theta_B)$. However, (3.5) shows that as $\theta_0 \to 0$ the dispersion relation will become singular. The simple message is to therefore stay away from the pole using the IT approximation.

TABLE 3. Percentage error of the wave frequencies calculated using the dispersion relation [(3.3)] and the polar-plane approximation in LeBlond (1964).

	$m = -1$	-2	-3	-4
$n = 1$	0.40	0.45	13.39	27.99
2	11.03	21.34	20.77	15.77
3	10.82	22.79	26.78	26.57
4	9.75	21.36	27.07	29.23
5	8.76	19.56	25.87	29.24

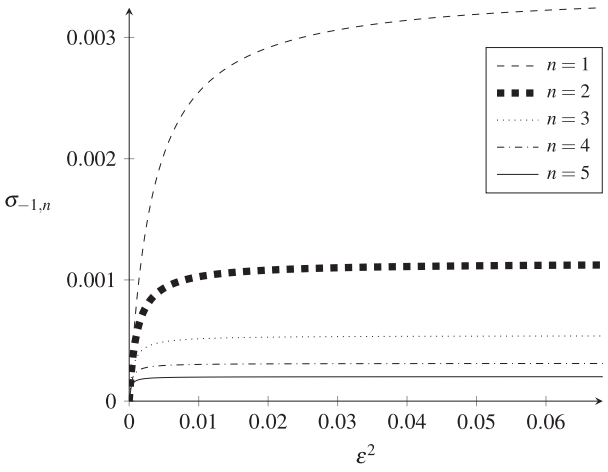

FIG. 2. Plot of the planetary waves frequencies $\sigma_{-1,n}$ $(n = 1, \ldots, 5)$ as a function of $\varepsilon^2 = (r_e/R)^2$ when $\theta_0 = 0.5\theta_B$.

4. Gravity waves ($\sigma > 1$)

For the high-frequency gravity modes, we rewrite the amplitude equation [(2.5a)] as

$$F'' + PF' + QF = 0, \tag{4.1}$$

where

$$P \equiv \frac{\sin 2\theta_0}{\cos^2\theta_0 - \sigma^2} + \cot\theta_0,$$

and

$$Q \equiv \left(\frac{R}{r_e}\right)^2 (\sigma^2 - \cos^2\theta_0) - \frac{m^2}{\sin^2\theta_0} - \frac{m}{\sigma}\left(\frac{\cos^2\theta_0 + \sigma^2}{\cos^2\theta_0 - \sigma^2}\right).$$

The meridional structure of the gravity modes is determined by the sign of $[(1/4)P^2 - Q]$. For given m, there exists σ_m^c such that

$$\begin{aligned}\mu^2 &\equiv (1/4)P^2 - Q \\ &= \frac{1}{4}\left(\frac{\sin 2\theta_0}{\cos^2\theta_0 - \sigma^2} + \cot\theta_0\right)^2 - \left(\frac{R}{r_e}\right)^2 (\sigma^2 - \cos^2\theta_0) \\ &\quad + \frac{m^2}{\sin^2\theta_0} + \frac{m}{\sigma}\left(\frac{\cos^2\theta_0 + \sigma^2}{\cos^2\theta_0 - \sigma^2}\right) > 0,\end{aligned}$$

TABLE 4. Sensitivity of the planetary wave eigenfrequencies to the choice of the colatitude θ_0, as measured by $|\sigma(0.75\theta_B) - \sigma(0.5\theta_B)|/\sigma(0.5\theta_B)$, expressed as a percentage.

	$m = -1$	-2	-3	-4
$n = 1$	21.85	51.95	75.58	90.77
2	6.59	19.8	36.24	52.09
3	3.04	9.74	19.39	30.44
4	1.73	5.69	11.74	19.25
5	1.12	3.71	7.79	13.06

when $1 < \sigma \le \sigma_m^c$. When $\sigma > \sigma_m^c$, the sign of μ^2 becomes negative. Following the method of solution in section 3, we obtain the gravity wave dispersion relation in a rotating polar cap:

$$\mu = \left(\frac{1}{2}P + \frac{m}{\sigma}\cot\theta_B\right)\tanh(\mu\theta_B), \tag{4.2a}$$

when $\mu^2 > 0$ (i.e., $1 < \sigma \le \sigma_m^c$). When $\sigma > \sigma_m^c$, the dispersion relation becomes

$$|\mu| = \left(\frac{1}{2}P + \frac{m}{\sigma}\cot\theta_B\right)\tan(|\mu|\theta_B). \tag{4.2b}$$

In the limit when $\sigma \gg 1$, $P \sim \cot\theta_0$, $Q \sim (R/r_e)^2\sigma^2$, and

$$\mu^2 \sim \left(\frac{1}{4}\right)\cot^2\theta_0 - \left(\frac{R}{r_e}\right)^2\sigma^2 \sim -\left(\frac{R}{r_e}\right)^2\sigma^2.$$

The dispersion relation [(4.2b)] can then be approximated, in this high-frequency limit, by

$$X = \frac{1}{2}\cot\theta_B \tan(X\theta_B), \tag{4.3}$$

where $X \equiv \sigma(R/r_e)$. This high-frequency gravity wave limit is, of course, captured by the f-sphere amplitude equation [(2.8)]. We observe from (4.3) that the gravity wave frequencies become independent of m in this limit. Table 5 presents the gravity wave mode frequencies using the basin parameters listed in Table 1. Table 5 indeed reveals that as $|m|$ increases the eigenfrequencies converge, namely, $\sigma_{m,n} \sim \sigma_{-m,n}$, as predicted by (4.3). The sensitivity of the gravity wave frequencies to θ_0 is again found to decrease with the increasing meridional modal number n. Figures 3 and 4

TABLE 5. Gravity wave frequencies calculated from (4.2) using the basin parameters in Table 1.

	$m = -4$	-3	-2	-1	1	2	3	4
$n = 1$	9.2928	7.0865	4.9357	2.9444	2.3844	4.5927	6.8469	9.1101
2	10.571	8.6917	7.0417	5.815	5.7373	6.9357	8.5877	10.478
3	12.74	11.228	10.004	9.1854	9.1546	9.9523	11.166	12.676
4	15.435	14.212	13.268	12.663	12.647	13.238	14.173	15.391
5	18.427	17.416	16.654	16.178	16.168	16.636	17.39	18.396

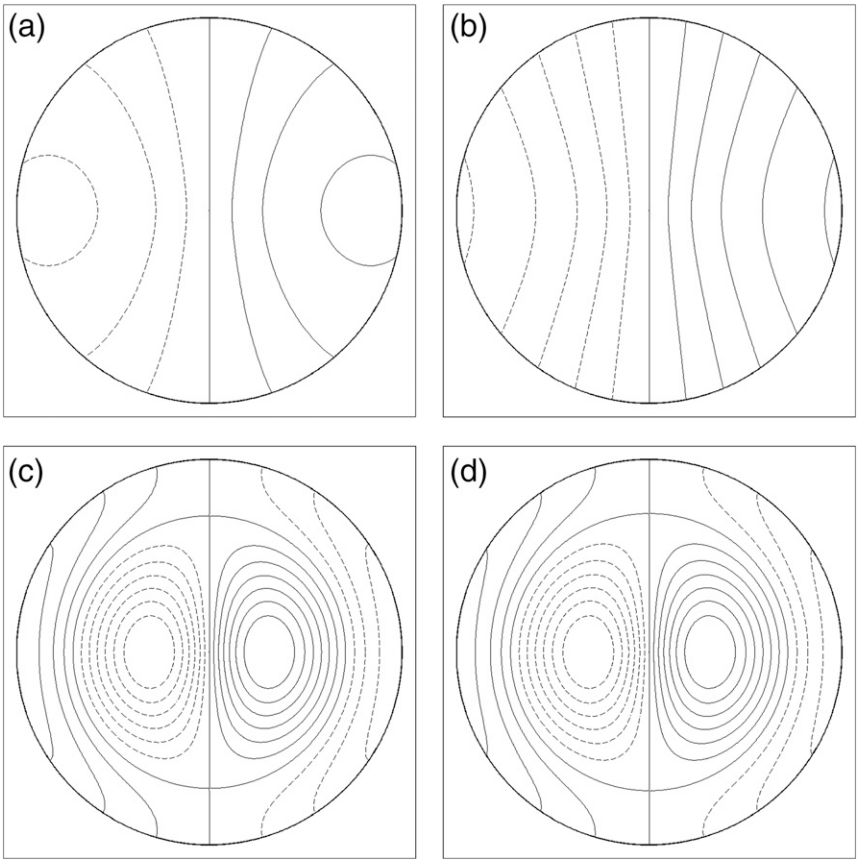

FIG. 3. Eigenfunctions associated with gravity wave modes. The dashed (solid) line represents negative (positive) values of sea surface elevation; (a) $\sigma_{-1,1}$, (b) $\sigma_{1,1}$, (c) $\sigma_{-1,2}$, and (d) $\sigma_{1,2}$. The patterns rotate counterclockwise (clockwise) for $m \geq 1 (m \leq -1)$.

show the normalized eigenfunctions proportional to the surface displacement for low-order gravity wave modes, $\sigma_{m,n}$ has $n - 1$ nodal circles of amplitude, and has $m + 1$ distinct cells in the azimuthal direction (i.e., m nodal diameters). The displacement field associated with the modes $\sigma_{m,1}$ ($m = \pm 1, \pm 2, \ldots$) resembles a coastal-trapped wave, with amplitude monotonically decreasing toward the center of the basin, although in the contrast with these vorticity waves, their propagation is not right bounded in the Northern Hemisphere.

Interestingly, the asymptotic behavior of the gravity wave frequencies when n is large can be deduced from the amplitude equation [(2.5a)] without invoking the IT approximation. First, observe that when $\sigma \gg 1$ (2.5a) can be approximated by

$$F'' + \cot\theta F' + \left(\frac{\sigma R}{r_e}\right)^2 F = 0. \tag{4.4}$$

The change of independent variable $z = \cos\theta$ transforms (4.4) into the ordinary differential equation

$$(1 - z^2)F'' - 2zF' + \left(\frac{\sigma R}{r_e}\right)^2 F = 0, \tag{4.5}$$

where $F' \equiv dF/dz$. Equation (4.5) is the Legendre equation, and it is well known that it supports bounded solutions on $[-1, 1]$ only when (see Abramowitz and Stegun 1965, their chapter 22)

$$\left(\frac{\sigma_n R}{r_e}\right)^2 = n(n+1). \tag{4.6}$$

In other words, the gravity wave eigenfrequencies become independent of m when $\sigma^2 \gg 1$, and (4.6) shows that

$$\sigma_n \sim \frac{r_e}{R} n \quad n \gg 1. \tag{4.7}$$

Similar asymptotic behavior for σ_n follows immediately from (4.3), where $\sigma_n \sim (r_e/R)(n\pi/\theta_B)$, where the difference in the constant of proportionality between this expression and (4.7) is due to the IT approximation.

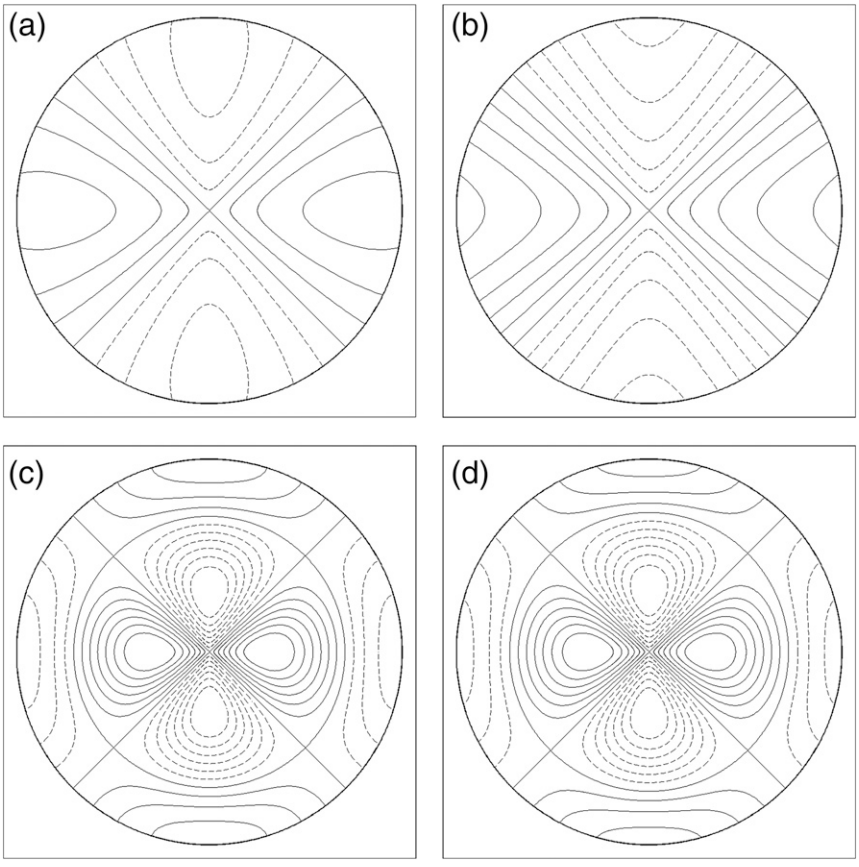

FIG. 4. As in Fig. 3, but for (a) $\sigma_{-2,1}$, (b) $\sigma_{2,1}$, (c) $\sigma_{-2,2}$, and (d) $\sigma_{2,2}$.

5. Conclusions and discussion

We have derived the governing amplitude equation for azimuthally propagating gravity and divergent planetary wave modes in a spherical cap, retaining full spherical geometry. Thereafter, we adopt the IT approximation first advanced by Imawaki and Takano (1974) and fixed the colatitude in the coefficients of the governing wave amplitude equation, thereby allowing analytical techniques to be used to solve the eigenvalue problem. The planetary wave frequencies calculated from the computationally efficient dispersion relation show acceptable agreement with their equivalent counterparts in LeBlond (1964) for relatively long azimuthal and meridional wavelength eigenfunctions. As these wavelengths decrease, the departure between the eigenfrequencies in LeBlond (1964) and in this study increases. This reflects the fact that short wavelength modes are more sensitive to the fixed value of the colatitude in the IT approximation. We have found that the gravest mode planetary wave eigenfrequency, which is accurately predicted by the dispersion relation derived using the IT approximation, is sensitive to the choice of the colatitude θ_0. Values of θ_0 other that $0.5\theta_B$ reduce the accuracy of this mode. The sensitivity of $\sigma_{m,n}$ to θ_0 reduces for $m = -1$ ($n = 2, \ldots, 5$), and for these frequencies the IT approximation produces an acceptable estimate of their exact value.

The eigenfrequencies and eigenfunctions (corresponding to the surface displacement) for gravity waves modes in a spherical polar cap are also calculated in this study. For a fixed azimuthal wavenumber $|m|$, there is a clockwise- and counterclockwise-propagating gravity wave mode, in contrast with the planetary waves. For fixed low values of m and n (the meridional wavenumber index), $\sigma_{-m,n} \neq \sigma_{m,n}$. However, as $|m|$ increases the frequencies of the clockwise- and counterclockwise-propagating modes converge in value, as predicted analytically in this study. Further, as n increases, $\sigma_{m,n}$ increases, and the dependence of $\sigma_{m,n}$ on m becomes weak. Asymptotically, we find that when $\sigma \gg 1, \sigma_{m,n} \propto n$, with dependence on m becoming weak.

The high degree of accuracy of the IT approximation in representing steady-state planetary flows in a spherical cap has been established by Kitauchi and Ikeda (2009). However, we are unaware of any study that

addresses how well the IT approximation captures freely propagating gravity and vorticity wave dynamics in a spherical cap, which is the purpose of this study. By fixing θ in the wave amplitude equation on a sphere, we are effectively assigning a fixed representative value of the meridional gradient of the Coriolis parameter. The resulting free-wave dynamics are in qualitative agreement with the planetary waves on a sphere, and for low modes there is also good quantitative agreement. For gravity modes at high frequencies (i.e., $\sigma \gg 1$), we demonstrate that σ is asymptotically in agreement, as a function of the meridional wavenumber n, with the equivalent expression derived using full spherical geometry. We anticipate that the low-order (long wavelength) planetary wave modes in a layered or a continuously stratified ocean in a polar cap will also be accurately represented using the IT approximation.

Acknowledgments. E. Gavilan gratefully acknowledges the support of a Newcastle University research studentship. We thank Miguel Morales Maqueda for his helpful comments on the presentation of the paper. We also thank two anonymous referees for their helpful and perceptive comments that have improved the final manuscript.

REFERENCES

Abramowitz, M., and I. A. Stegun, Eds., 1965: *Handbook of Mathematical Functions*. Dover Publications, 1046 pp.

Bridger, A. F. C., and D. E. Stevens, 1980: Long atmospheric waves and the polar-plane approximation to the Earth's spherical geometry. *J. Atmos. Sci.*, **37**, 534–544, doi:10.1175/1520-0469(1980)037<0534:LAWATP>2.0.CO;2.

Harlander, U., 2005: A high-latitude quasi-geostrophic delta plane model derived from spherical geometry. *Tellus*, **57A**, 43–54, doi:10.3402/tellusa.v57i1.14601.

Haurwitz, B., 1975: Long circumpolar atmospheric waves. Arch. Meteor. *Geophys. Bioklimatol.*, **24A**, 1–18, doi:10.1007/BF02247554.

Imawaki, S., and K. Takano, 1974: Planetary flow in a circular basin. *Deep-Sea Res. Oceanogr. Abstr.*, **21**, 69–76, doi:10.1016/0011-7471(74)90020-5.

Kitauchi, H., and M. Ikeda, 2009: An analytic solution of steady Stokes flow on a rotating polar cap. *Fluid Dyn. Res.*, **41**, 045505, doi:10.1088/0169-5983/41/4/045505.

LeBlond, P. H., 1964: Planetary waves in a symmetrical polar basin. *Tellus*, **16**, 503–512, doi:10.3402/tellusa.v16i4.8989.

Longuet-Higgins, M. S., 1968: The eigenfunctions of Laplace's tidal equations over a sphere. *Philos. Trans. Roy. Soc. London*, **A262**, 511–607, doi:10.1098/rsta.1968.0003.

Paldor, N., 2015: *Shallow Water Waves on the Rotating Earth*. Springer, 77 pp.

——, Y. De-Leon, and O. Shamir, 2013: Planetary (Rossby) waves and inertia–gravity (Poincaré) waves in a barotropic ocean over a sphere. *J. Fluid Mech.*, **726**, 123–136, doi:10.1017/jfm.2013.219.